Circumventing the Manley-Rowe Quantum Efficiency Limit in an Optically Pumped Terahertz Quantum-Cascade Amplifier

Inès Waldmueller,[1,*] Michael C. Wanke,[1] and Weng W. Chow[1,2]

[1]*Sandia National Laboratories, Albuquerque, New Mexico 87185-1086, USA*

[2]*Physics Department and Institute of Quantum Studies, Texas A&M University, College Station, Texas 77843, USA*

(Received 6 November 2006; published 14 September 2007)

Using a microscopic theory based on the Maxwell-semiconductor Bloch equations, we investigate the feasibility of an optically pumped electrically driven terahertz (THz) quantum-cascade laser as a pathway to room-temperature THz generation. In optical conversion schemes the power conversion efficiency is limited by the Manley-Rowe relation. We circumvent this constraint by incorporating an electrical bias in a four level intersubband scheme, thereby allowing coherent recovery of the optical pump energy. The observed THz radiation is generated through both stimulated emission and automatically phase-matched quantum coherence contributions—making the proposed approach both a promising source for THz radiation and a model system for quantum coherence effects such as lasing without inversion and electromagnetically induced transparency.

DOI: 10.1103/PhysRevLett.99.117401 PACS numbers: 78.67.De, 42.65.Wi, 68.65.Fg

Quantum-cascade lasers (QCLs) have become an important topic during the past decade. Based on transitions between conduction subbands, QCLs have been fabricated for a wide range of infrared frequencies. Recently, significant interest has focused on the development of QCLs in the terahertz (THz) regime [1]. In the conventional THz-QCL, carriers are injected directly into the energetically higher laser subband. The lower laser subband is depleted by zero, single, or double optical-phonon scattering [1–3], and for low temperatures population inversion between the lasing subbands can be obtained. With increasing temperature, however, increasing nonradiative relaxation channels and thermal backfilling detrimentally affect the population inversion. As a result, the lasing threshold of direct QCLs in the THZ regime increases appreciably with increasing temperature, limiting the present maximum operation temperature to 164 K for pulsed and 112 K for continuous-wave (cw) operation [4].

Optical conversion is one approach to simultaneously reducing the problem of both parasitic current channels and thermal backfilling. It offers the possibility to (i) locate the lasing subbands energetically high enough to prevent thermal backfilling and (ii) to decrease the amount of parasitic current channels due to a reduced coupling between the lasing and the surrounding subbands. Instead of electrical pumping, optical pumping is used to populate the upper laser subband, and THz radiation is obtained either via stimulated emission or by exploiting electron Raman scattering (e.g., [5,6] or recently [7]). However, while conventional optical conversion presents a solution to the problem of population thermalization, it also introduces a fundamental constraint due to the Manley-Rowe quantum limit. The highest achievable conversion efficiency is given by the quotient of output and input frequencies; i.e., for far-infrared (FIR) to THz conversion this translates into a maximum conversion efficiency of ≈10%–15%. Additionally, optical conversion schemes based on second order nonlinear mixing (e.g., [8–10]) have the disadvantage of phase-matching constraints.

In this Letter, we propose and model an optically pumped electrically driven quantum-cascade laser. In contrast to optical conversion schemes, the THz energy is not derived from the external optical field, but comes from the forward electrical bias as in a conventional QCL. In this way our approach is similar to recently proposed designs for THz generation using Bloch oscillations in superlattices [11,12]. However, in contrast to [11,12], our design allows the coherent recovery of the pump field. Therefore, we get the advantages of an optical conversion scheme, but circumvent the constraint of the Manley-Rowe limit. Furthermore, the proposed scheme not only generates THz radiation via stimulated emission, but also from automatically phase-matched quantum coherence contributions. The basic features of our approach are sketched in Fig. 1. The novelty of the approach is the design of the

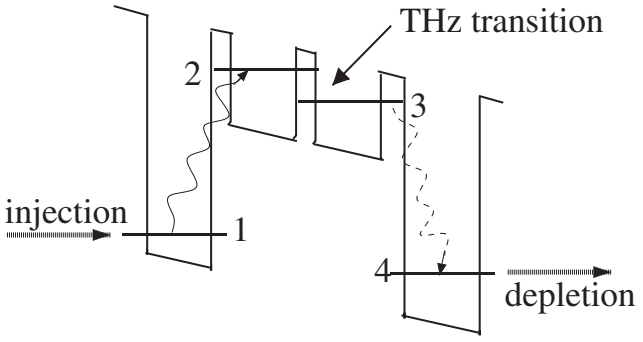

FIG. 1. Single stage of proposed optically pumped electrically driven QCL. Without pump recovery (dashed transition), the scheme reverts to a conventional optical conversion configuration.

coupled quantum wells so that the transition frequencies between subbands 1 and 2 and subbands 3 and 4 are sufficiently similar for an external optical field to simultaneously populate the higher laser subband (2) and deplete the lower laser subband (3), thus regaining the pump photons via stimulated emission.

In the following, we demonstrate the capabilities of the scheme theoretically by investigating the intensities of the involved optical fields, i.e., the THz field and the pump field, using Maxwell's wave equations:

$$\left(\nabla^2 + \frac{n^2}{c^2}\frac{\partial^2}{\partial t^2}\right)\mathcal{E}_i(r,t) = -\mu_0 \frac{\partial^2}{\partial t^2}\mathcal{P}_i(r,t). \quad (1)$$

In Eq. (1), $\mathcal{E}_i(r,t) = \tilde{\mathcal{E}}_i(r,t)e^{-i\omega_i t}$ + c.c. denotes THz (i = THz) and pump ($i = P$) field with complex amplitudes $\tilde{\mathcal{E}}_i(r,t)$. The material response has been divided into a nonresonant part, lumped in with the (background) refractive index n, and a resonant part, treated dynamically in terms of the macroscopic optical polarization $\mathcal{P}_i(r,t)$. The latter is composed of the respective microscopic polarizations P_{ab} between subbands a and b

$$\mathcal{P}_{\mathrm{THz}} = (d_{14}P_{14} + d_{23}P_{32}) + \text{c.c.}, \quad (2)$$

$$\mathcal{P}_P = (d_{12}P_{21} + d_{34}P_{34}) + \text{c.c.}, \quad (3)$$

which are calculated within the framework of the semiconductor Bloch equations:

$$\frac{d}{dt}P_{ab} = \left(\frac{i}{\hbar}E_{ab} - \gamma\right)P_{ab} + \frac{i}{\hbar}d_{ab}(n_a - n_b)(\mathcal{E}_{\mathrm{THz}} + \mathcal{E}_P) + \frac{i}{\hbar}\sum_{\substack{c=1 \\ c\neq a,b}}^{4}(d_{bc}P_{ac} - d_{ac}P_{cb})(\mathcal{E}_{\mathrm{THz}} + \mathcal{E}_P) \quad (4)$$

$$\frac{d}{dt}n_a = \frac{i}{2\hbar}\sum_{\substack{c=1 \\ c\neq a}}^{4} d_{ca}(P_{ca} - P_{ac})(\mathcal{E}_{\mathrm{THz}} + \mathcal{E}_P) + \frac{d}{dt}n_a\Big|_s. \quad (5)$$

d_{ab} is the dipole moment and E_{ab} the transition energy between subbands a and b, determined self-consistently within a Schrödinger-Poisson solver. n_a denotes the population of subband a, γ the dephasing rate of the polarizations, and $\frac{d}{dt}n_a|_s$ accounts for population relaxation effects due to carrier-carrier and carrier-phonon scattering. These contributions are taken into account with microscopically determined scattering rates (for details see, e.g., [13]). Equation (4) shows the dependence of the polarizations on two distinct contributions: (I) stimulated emission or absorption (population dynamics) and (II) quantum coherence effects (microscopic polarization interference). Quantum coherence effects, caused by quantum interference of different channels of radiative processes, were first observed in atomic systems. In our system, the influence on the THz field from polarizations induced by dipole-forbidden transitions ($1 \leftrightarrow 3$ and $2 \leftrightarrow 4$) offers the possibility of absorption cancellation without emission cancellation. As a result, effects such as electromagnetically induced transparency (EIT) and lasing without inversion (LWI) can be observed (for a textbook discussion see, e.g., [14]). We will show in the following discussion that both stimulated emission and quantum coherence contributions can give rise to a substantial amount of THz radiation in the proposed QCL.

We evaluate the general capabilities of the proposed scheme for the example of an AlGaAs/GaAs structure with a sheet carrier density of $N = 3 \times 10^{11}$ cm^{-2}, operated at a lattice temperature of $T = 220$ K. The relevant transition energies, dipole moments, and lifetimes are calculated as $E_{21} = E_{34} = 144$ meV, $E_{23} = 16$ meV, $d_{12} = d_{34} = 1.5$ nm, $d_{23} = 4$ nm, $\tau_{21} = 4.4$ ps, $\tau_{23} = 1.2$ ps, and $\tau_{34} = 5.7$ ps. From our quantum kinetic calculations we determine the dephasing rate for the THz transition as $\gamma = 2.5$ ps^{-1}, which agrees with the experimental results presented in [15]. The total loss consisting of contributions from waveguide, mirror, and free carrier absorption is estimated to be $\alpha_{\mathrm{THz}} = 140$ cm^{-1} for the THz field and $\alpha_{\mathrm{FIR}} = 50$ cm^{-1} for the pump field.

First, we investigate the benefits of the coherent recycling of the pump. Figure 2 shows the response of the structure to optical excitation with a Gaussian pulse (temporal width $\sigma = 30$ ps, peak pump intensity $I_{\mathrm{PP}} = 16.5$ MW/cm^2) which spatially propagates perpendicular to the growth direction; i.e., the pulse propagates in the quantum-well-in-plane direction x. A comparison of the depletion of the pump field and the resulting buildup of THz radiation with (solid lines) and without (dashed lines) pump recycling shows that pump recycling yields a

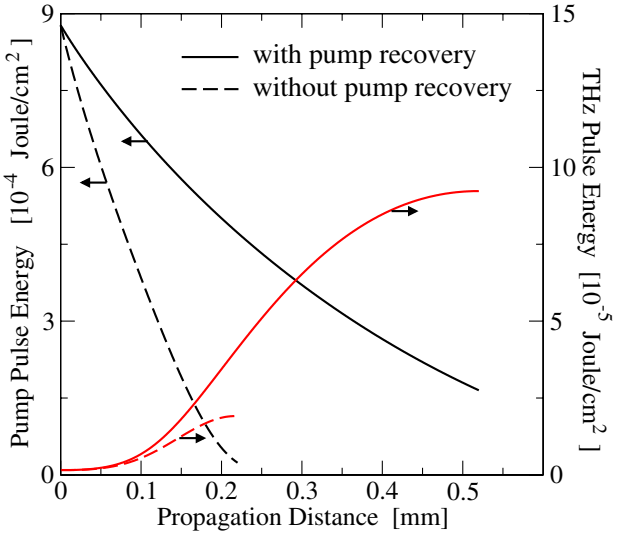

FIG. 2 (color online). Spatial response (at 220 K) to pulse excitation propagating in the quantum-well-in-plane direction for a design with pump recycling (solid lines) and without pump recycling (dashed lines). A 5 times enhanced conversion efficiency is achieved from coherent pump recovery.

strongly increased propagation length, resulting in an enhanced gain of THz radiation. As a figure of merit for the general feasibility of the scheme and the benefits of the pump recycling, we investigate the optical conversion efficiency η, which is the ratio of maximum output over input (i.e., THz pulse energy over pump pulse energy for pulse excitation and THz intensity over pump intensity for cw excitation, respectively). For the example presented in Fig. 2, with recycling we achieve an optical conversion efficiency of $\eta = 10.3\%$, while without recovery of the pump energy we achieve an optical conversion efficiency of only $\eta = 2\%$. Thus, recycling the pump energy increases the optical conversion efficiency for this example by a factor of 5.

Next, we examine the dependence of the optical conversion efficiency on the pump energy for (a) excitation with a 3 ps pulse, (b) excitation with a 30 ps pulse, and (c) - continuous-wave excitation (cf. Fig. 3). A comparison of the predicted conversion efficiencies shows a strong dependence on the excitation duration. As the generation of THz radiation is not only due to stimulated emission, but also to quantum coherence contributions, i.e., interference of generated polarizations, the buildup of THz radiation can increase with increasing excitation duration. The highest optical conversion efficiencies are observed for cw excitation. For completeness, we present in the inset of Fig. 3 the (cw) optical conversion efficiencies for operation at different lattice temperatures, $T = 150$, 220, and 300 K, all of which are higher than the highest operational temperature achieved for (cw) THz-QCLs to date.

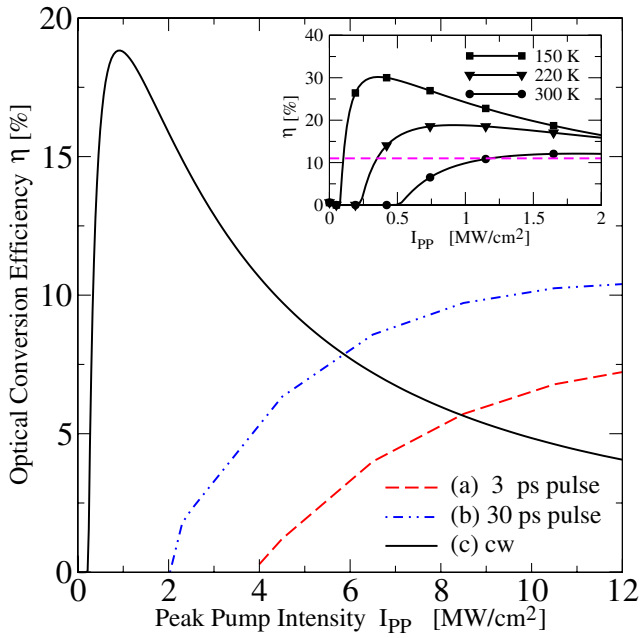

FIG. 3 (color online). Dependence of optical conversion efficiency on peak pump intensity I_{PP} at 220 K for (a) excitation with a 3 ps pulse, (b) excitation with a 30 ps pulse, and (c) continuous-wave excitation. The inset shows the temperature dependence of the optical conversion efficiency for cw excitation, demonstrating the possibility to exceed the Manley-Rowe limit (dashed line).

We find that for weak excitation, the optical conversion efficiency increases with increasing peak pump intensity. However, for higher peak pump intensities the THz gain slowly saturates due to a combination of both optical Stark effect and pump-induced population redistribution (similar to the saturation predicted for optically pumped semiconductor quantum wells in [16]). As a result, the optical conversion efficiency is maximized for an optimal pump intensity which can be clearly seen for the example of cw operation in Fig. 3.

Because of temperature-dependent nonradiative carrier recombination and dephasing of the polarizations, the highest achievable optical conversion efficiency and the width of the window for optimal pump intensity are also temperature dependent (cf. inset of Fig. 3) yielding a decrease of optical conversion efficiency with increasing temperature. However, even for room-temperature operation our approach predicts promising optical conversion efficiencies.

Last, we present in Fig. 4 the dependence of the modal amplitude THz gain on the detuning of a weak THz-probe field from the lasing transition, $\delta_\omega = \hbar\omega_{\mathrm{THz}} - (E_2 - E_3)$. Table I gives an overview of the corresponding pump intensities and relative populations of the various subbands for the considered cases pictured in Fig. 4. For excitation with a small cw-pump field (case A), population inversion between the lasing subbands is not obtained and there is only absorption. However, with increasing pump intensity, we observe the onset of quantum coherence effects: EIT and then LWI in cases B and C, respectively. Numerical simulations showed no phase-matching requirement. We confirm this result analytically by solving the Bloch equations for resonant continuous-wave excitation and negli-

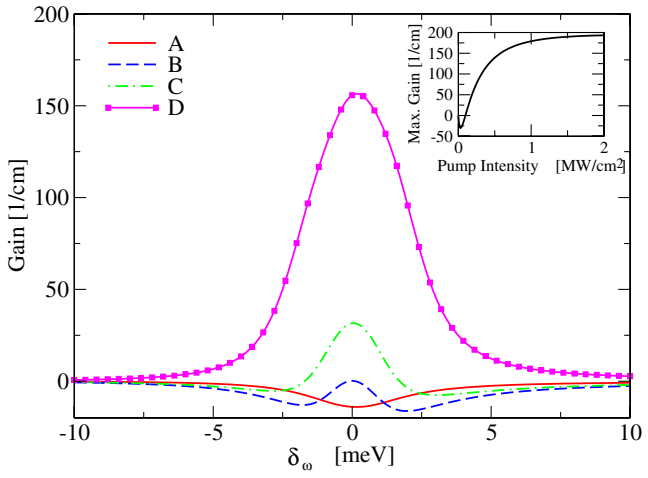

FIG. 4 (color online). Modal amplitude gain (half of intensity gain) at 220 K as function of THz-probe detuning and pump intensity.

TABLE I. Pump intensity and relative steady-state populations of subbands 1–4 for cases A–D of Fig. 4.

	I_P (MW/cm^2)	n_1/N	n_2/N	n_3/N	n_4/N
A	0.006	0.93	0.026	0.041	0.003
B	0.098	0.63	0.162	0.189	0.019
C	0.151	0.582	0.194	0.198	0.026
D	0.631	0.479	0.301	0.167	0.053

gible resonant THz-probe field. Expressing the polarization of the THz transition solely in terms of the steady-state populations of subbands 1–4 gives

$$\mathrm{Im}\,(P_{32}) = \left[\frac{(n_2 - n_3)\gamma}{2(|\tilde{\Omega}_P|^2 + \gamma^2)} + \frac{|\tilde{\Omega}_P|^2(n_1 + n_2 - n_3 - n_4)}{8\gamma(|\tilde{\Omega}_P|^2 + \gamma^2)}\right]\tilde{\Omega}_{\mathrm{THz}}. \quad (6)$$

In Eq. (6), γ denotes the dephasing time of the intersubband coherences, n_1–n_4 the steady-state populations of subbands 1–4 (which depend on the intensity of the pump field), and $\tilde{\Omega}_i = \hbar^{-1} d_i \tilde{\mathcal{E}}_i$ the Rabi frequency of field $\tilde{\mathcal{E}}_i$. Note that for simplicity, we give only the explicit result for the special case of an optically pumped electrically driven QCL with $d_{12} \equiv d_{34} = d_P$.

The first term in Eq. (6) accounts for the possible generation of THz radiation via stimulated emission; thus, this contribution only yields THz gain if there is a population inversion. The second term in Eq. (6) accounts for quantum coherence contributions and can give rise to THz gain whenever the subband populations fulfill the condition $n_1 + n_2 - n_3 - n_4 > 0$, which allows lasing without population inversion. For the design presented in Fig. 1, all sources of THz radiation in Eq. (6) depend on the pump field only through its intensity and are consequently automatically phase matched to the THz field. For cases A–C of Fig. 4, population inversion between the lasing subbands (subband 2 and subband 3) does not exist; thus, the observed gain is due to the second term in Eq. (6), i.e., quantum coherence contributions. Finally, in case D, population inversion is obtained and stimulated emission also contributes to the THz gain. However, the necessary population condition for the quantum coherence contributions is fulfilled as well. Thus, both stimulated emission and quantum coherence simultaneously contribute to the THz gain. Evaluating Eq. (6) for the parameters of case D shows that at zero detuning both mechanisms contribute roughly equally to the THz gain. The inset of Fig. 4 shows the dependence of the maximum modal gain on the pump intensity. With increasing pump intensity, the gradual saturation of the pump-induced population redistribution and the onset of the optical Stark effect yield a saturation of the modal gain.

In conclusion, we have proposed an optically pumped electrically driven quantum-cascade laser as a new approach for THz generation. Theoretical investigations showed promising optical conversion efficiencies for both pulsed and cw excitation for a broad temperature range up to 300 K. The predicted efficiencies can dramatically exceed the Manley-Rowe quantum limit due to coherent recycling of the pump field. For weak excitation the optical conversion efficiency increases with increasing peak pump intensity, while for strong excitation the optical conversion efficiency decreases due to a saturation of the modal gain leaving a temperature-dependent window for optimal pump excitation. Calculated gain spectra demonstrated that both stimulated emission and automatically phase-matched quantum coherence contributions can give rise to THz radiation. As a result, the approach is not only a promising source for THz generation at high temperatures, but also an interesting model system for investigating quantum coherence effects such as electromagnetically induced transparency and lasing without inversion.

This work is funded by the U.S. Department of Energy under Contract No. DE-AC04-94AL8500 and the Alexander von Humboldt Foundation.

*iwaldmu@sandia.gov

[1] R. Koehler *et al.*, Nature (London) **417**, 156 (2002).
[2] B. S. Williams *et al.*, Appl. Phys. Lett. **82**, 1015 (2003).
[3] B. S. Williams *et al.*, Appl. Phys. Lett. **88**, 261101 (2006).
[4] B. Williams *et al.*, Opt. Express **13**, 3331 (2005).
[5] O. Gauthier-Lafaye *et al.*, Appl. Phys. Lett. **74**, 1537 (1999).
[6] H. C. Liu *et al.*, Phys. Rev. Lett. **90**, 077402 (2003).
[7] M. Troccoli *et al.*, Nature (London) **433**, 845 (2005).
[8] N. Owschimikow *et al.*, Phys. Rev. Lett. **90**, 043902 (2003).
[9] C. Gmachl *et al.*, IEEE J. Quantum Electron. **39**, 1345 (2003).
[10] S. S. Dhillon *et al.*, Appl. Phys. Lett. **87**, 071101 (2005).
[11] Y. Shimada *et al.*, Phys. Rev. Lett. **90**, 046806 (2003).
[12] A. Zhang *et al.*, Appl. Phys. Lett. **86**, 171110 (2005).
[13] I. Waldmueller *et al.*, IEEE J. Quantum Electron. **42**, 292 (2006).
[14] M. O. Scully and M. S. Zubairy, *Quantum Optics* (Cambridge University Press, Cambridge, England, 1997).
[15] R. Ascazubi *et al.*, Appl. Phys. Lett. **81**, 4344 (2002).
[16] A. Liu and C. Z. Ning, Appl. Phys. Lett. **75**, 1207 (1999).